UV-B photoreceptor-mediated protection of the photosynthetic machinery in *Chlamydomonas reinhardtii*

Guillaume Allorent[a], Linnka Lefebvre-Legendre[a], Richard Chappuis[a], Marcel Kuntz[b], Thuy B. Truong[c,d], Krishna K. Niyogi[c,d], Roman Ulm[a,e,1], and Michel Goldschmidt-Clermont[a,e,1]

[a]Department of Botany and Plant Biology, Sciences III, University of Geneva, Geneva CH-1211, Switzerland; [b]Laboratoire de Physiologie Cellulaire et Végétale, Commissariat à l'Énergie Atomique et aux Énergies Alternatives/Centre National de la Recherche Scientifique/Université Grenoble Alpes/Institut National de la Recherche Agronomique, 38054 Grenoble, France; [c]Howard Hughes Medical Institute, Department of Plant and Microbial Biology, University of California, Berkeley, CA 94720; [d]Molecular Biophysics and Integrated Bioimaging Division, Lawrence Berkeley National Laboratory, Berkeley, CA 94720; and [e]Institute of Genetics and Genomics of Geneva, University of Geneva, Geneva CH-1211, Switzerland

Edited by Elisabeth Gantt, University of Maryland, College Park, MD, and approved November 11, 2016 (received for review May 13, 2016)

Life on earth is dependent on the photosynthetic conversion of light energy into chemical energy. However, absorption of excess sunlight can damage the photosynthetic machinery and limit photosynthetic activity, thereby affecting growth and productivity. Photosynthetic light harvesting can be down-regulated by nonphotochemical quenching (NPQ). A major component of NPQ is qE (energy-dependent nonphotochemical quenching), which allows dissipation of light energy as heat. Photodamage peaks in the UV-B part of the spectrum, but whether and how UV-B induces qE are unknown. Plants are responsive to UV-B via the UVR8 photoreceptor. Here, we report in the green alga *Chlamydomonas reinhardtii* that UVR8 induces accumulation of specific members of the light-harvesting complex (LHC) superfamily that contribute to qE, in particular LHC Stress-Related 1 (LHCSR1) and Photosystem II Subunit S (PSBS). The capacity for qE is strongly induced by UV-B, although the patterns of qE-related proteins accumulating in response to UV-B or to high light are clearly different. The competence for qE induced by acclimation to UV-B markedly contributes to photoprotection upon subsequent exposure to high light. Our study reveals an anterograde link between photoreceptor-mediated signaling in the nucleocytosolic compartment and the photoprotective regulation of photosynthetic activity in the chloroplast.

nonphotochemical quenching | UV-B photoreceptor | PSBS | LHCSR1 | photoprotection

Light is essential for photosynthesis, but absorption of excess light energy is detrimental. To avoid photodamage, photosynthetic light harvesting is regulated by nonphotochemical quenching (NPQ), which allows dissipation of harmful excess energy as heat through its qE (energy-dependent nonphotochemical quenching) component (1–6). Specialized members of the light harvesting complex (LHC) protein family, such as Photosystem II Subunit S (PSBS) in higher plants or members of the LHC Stress-Related (LHCSR) family in mosses and algae, are central to qE (7–11). Protonation of key residues in these proteins triggers qE in response to the acidification of the thylakoid lumen, which is coupled to photosynthetic electron transport (7, 9). Furthermore, the deepoxidation of violaxanthin to zeaxanthin, which is also activated by the acidification of the thylakoid lumen, enhances qE (12). In response to high levels of visible light, LHCSR3 protein accumulation is of major importance for qE capacity in *Chlamydomonas reinhardtii* (11). The induction of *LHCSR3* expression under high light is thought to involve retrograde signaling, from the chloroplast to nuclear gene expression (13), and recent data show that the response is also dependent on the phototropin (PHOT) blue light photoreceptor (14).

UV-B radiation is intrinsic to sunlight reaching the earth surface and is potentially damaging to living tissues. UV-B stress tolerance is induced through the specific activation of acclimation responses (15–20). Plants sense UV-B radiation via the homodimeric UV-B photoreceptor UV Resistance Locus 8 (UVR8) (21–23) that is mainly localized in the cytosol (24). Absorption of UV-B photons by intrinsic tryptophan residues leads to UVR8 monomerization, interaction with the E3 ubiquitin ligase Constitutively Photomorphogenic 1 (COP1), accumulation in the nucleus, and changes in gene expression (19, 21–29). After photoreception, UVR8 returns to the homodimeric ground state by redimerization (30, 31). The UVR8–COP1 pathway is evolutionarily conserved and induces UV-B acclimation and protection in *Chlamydomonas* (32).

Photodamage is associated with the UV-B part of the sunlight spectrum (33, 34). In both *Arabidopsis* and *Chlamydomonas*, some of the UV-B–induced genes encode chloroplast proteins, and UV-B acclimation allows maintenance of photosynthetic efficiency under elevated levels of UV-B (32, 35). However, a direct mechanistic link between UVR8 photoreceptor signaling and photoprotection of the photosynthetic machinery has remained unknown. Here, we describe a distinct qE response in *Chlamydomonas* that is based on direct UV-B reception by UVR8, which, together with COP1, initiates anterograde signaling and the chloroplastic accumulation of LHCSR and PSBS proteins and results in the protection of the photosynthetic machinery.

Significance

Life on earth largely depends on the capture of light energy by plants through photosynthesis. Light is essential, but excess light is dangerous. Energy dissipation as heat is a major mechanism induced to protect the photosynthetic machinery. We report that UV-B perception by a specific photoreceptor in the nucleocytosolic compartment leads to protection of the photosynthetic machinery in the chloroplast of a green alga. The underlying mechanism is markedly different from the response to high light. UV-B photoreceptor-mediated signaling activates a safety valve, allowing the release of the excess energy as heat, helping the algae to cope with too much light energy.

Author contributions: G.A., R.U., and M.G.-C. designed research; G.A., L.L.-L., R.C., and M.K. performed research; T.B.T. and K.K.N. contributed new reagents/analytic tools; G.A., L.L.-L., R.C., M.K., R.U., and M.G.-C. analyzed data; and G.A., R.U., and M.G.-C. wrote the paper.

The authors declare no conflict of interest.

This article is a PNAS Direct Submission.

Freely available online through the PNAS open access option.

[1]To whom correspondence may be addressed. Email: roman.ulm@unige.ch or michel.goldschmidt-clermont@unige.ch.

This article contains supporting information online at www.pnas.org/lookup/suppl/doi:10.1073/pnas.1607695114/-/DCSupplemental.

Results and Discussion

A recent transcriptome analysis revealed that nuclear-encoded *PSBS*, *LHCSR1*, and *LHCSR3* transcripts accumulate in *Chlamydomonas* exposed to a low dose of UV-B (32). We thus tested whether the respective proteins accumulate under this condition, which induces UV-B acclimation and tolerance (32). Indeed, we found that UV-B induced a marked accumulation of the PSBS and LHCSR1 proteins and, to a lesser extent, LHCSR3 (Fig. 1*A*). This pattern was strikingly distinct from the high-light response (350 $\mu mol \cdot m^{-2} \cdot s^{-1}$), when LHCSR3 accumulated strongly, LHCSR1 accumulated less, and PSBS was undetectable (Fig. 1*B*). At higher light intensity (900 $\mu mol \cdot m^{-2} \cdot s^{-1}$), PSBS expression was detectable (Fig. S1) (36, 37), although at lower levels than under UV-B (Fig. S1). In the *npq4* mutant deleted for the *LHCSR3* genes *LHCSR3.1* and *LHCSR3.2* that encode identical proteins (11), UV-B induction of LHCSR1 and PSBS was comparable to the wild type (WT) (Fig. 1*A*). Interestingly, UV-B–responsive accumulation of LHCSR1 and PSBS proteins was not affected by treatment with the photosystem II (PSII) inhibitor dichlorophenyl-dimethylurea (DCMU), in sharp contrast to LHCSR3 under high light (Fig. 1*C*). Thus, induction of LHCSR1 and PSBS by UV-B does not depend on photosynthetic electron transfer, unlike LHCSR3 induction under high light (38). We conclude that UV-B and high light induce clearly distinct patterns of expression of qE-related proteins.

The marked accumulation of PSBS and LHCSR1 prompted us to test whether UV-B indeed increases qE capacity. NPQ includes qE and state transition (qT), which lead to rather complex kinetics of chlorophyll fluorescence upon exposure of *Chlamydomonas* to high light (Fig. S2) (39). We used nigericin to abolish the proton gradient and specifically quantify the qE component of NPQ (Fig. 2 *A–D*) (12, 39). Indeed, a clear nigericin-sensitive qE was observed in WT cells preexposed to low levels of UV-B for 6 h (Fig. 2 *A* and *E* and Fig. S3*A*). Another feature characteristic of qE was rapid relaxation upon returning to the dark condition (Fig. S3). qE capacity developed already after 2 h of UV-B exposure, and after 6 h of UV-B, it was similar to qE after 6 h of high-light exposure (Fig. 2*E*). These data clearly indicate that exposure to UV-B induces qE capacity in *Chlamydomonas*.

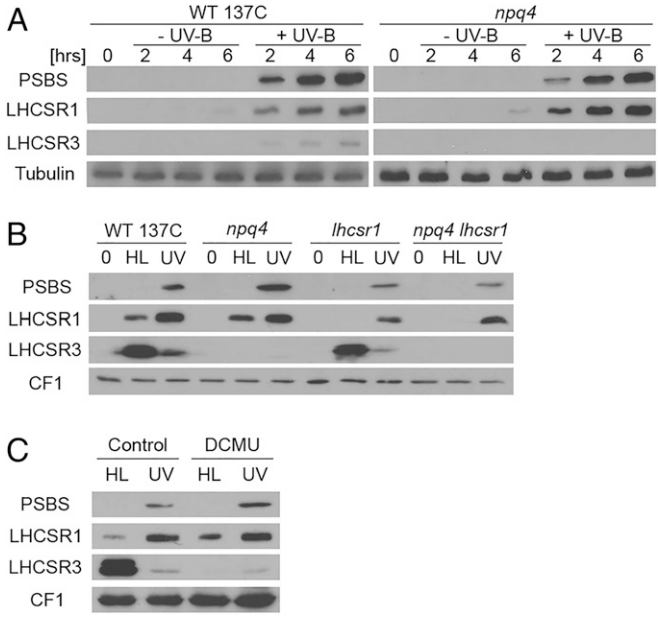

Fig. 1. UV-B and high light induce distinct patterns of qE-related proteins. (*A*) Immunoblot analysis of PSBS, LHCSR1, and LHCSR3 protein levels in the WT (WT 137C) and *npq4* mutant exposed to UV-B (+UV-B) for 2, 4, and 6 h or not exposed (−UV-B; protected by a UV-B–absorbing long-pass filter). Tubulin levels are shown as loading control. (*B*) Immunoblot analysis of PSBS, LHCSR1, and LHCSR3 protein levels in WT, *npq4*, *lhcsr1*, and *npq4 lhcsr1* before treatment (0) and after exposure for 6 h to high light (HL) or to UV-B (UV). (*C*) Immunoblot analysis of PSBS, LHCSR1, and LHCSR3 protein levels in WT in the presence or absence of the photosynthetic electron transport inhibitor dichlorophenyl-dimethylurea (DCMU; 5 μM). (*B* and *C*) ATPase (CF1) levels are shown as loading control.

The marked accumulation of PSBS and LHCSR1 suggested that qE induced by UV-B is partly independent of LHCSR3. Consistently, a clear UV-B–induced qE component was observed in the LHCSR3-deficient *npq4* mutant (Fig. 2 *B* and *F* and Fig. S3*A*), albeit with an amplitude (qE = 0.65 ± 0.04; $n = 3$) lower than in WT (qE = 1.01 ± 0.06; $n = 3$) (Fig. 2 *E* and *F*). In contrast, *npq4* cells exposed to high light for 6 h showed no significant induction of qE (Fig. 2 *D* and *F* and Fig. S3*B*). Thus, we conclude that part of the qE capacity induced by UV-B is not dependent on LHCSR3, which raises the possibility that PSBS or LHCSR1 or both together may contribute to qE.

We then tested induction of qE capacity in the mutant *lhscr1* and the double-mutant *npq4 lhcsr1*, the latter of which is strongly impaired in qE after exposure to high light (7). *lhcsr1* carries a point mutation in the coding sequence that substitutes tyrosine-164 for asparagine (Y164N). $LHCSR1^{Y164N}$ accumulated in lower amounts in *lhcsr1* than LHCSR1 in the WT after UV-B treatment (Fig. 1*B*). Nonetheless, qE was much lower in *lhcsr1* than in *npq4* after UV-B exposure (Fig. 2*G*). This finding is in support of a major role for LHCSR1 in UV-B–induced qE capacity. Conversely, after exposure to high light, a comparison of *npq4* and *lhcsr1* showed that LHCSR3 was a main agent of qE, but that LHCSR1 also contributed (Fig. 2*G*) (40). In stark contrast to the absence of qE in response to high light, qE in the double-mutant *npq4 lhcsr1* after UV-B exposure was clearly detectable and similar to *lhcsr1* (Fig. 2*G* and Fig. S3*A*). This finding may indicate PSBS activity in the absence of LHCSR3 and LHCSR1, although we cannot exclude the possibility that $LHCSR1^{Y164N}$ retains some activity. We conclude that LHCSR1 and possibly PSBS are key effectors after UV-B treatment, whereas LHCSR3 is the major active agent after high-light exposure.

PSBS activity in response to high light has been reported only very recently in *Chlamydomonas* (36, 37). To investigate a possible contribution of PSBS to qE after UV-B exposure, we tested whether constitutive expression of PSBS in the *Chlamydomonas* chloroplast enhances qE in the *npq4* mutant background (Fig. S4). The overexpression of PSBS increased the amplitude of qE in the *npq4* mutant after UV-B exposure (Fig. S4 *H* and *I*). Thus, in agreement with two recent reports (36, 37), PSBS is functional in *Chlamydomonas* and may contribute to qE activity in response to UV-B.

Under high light, qE is enhanced by the deepoxidation of violaxanthin to zeaxanthin (12), both of which are bound by LHCSR3 (8). After UV-B exposure, the level of violaxanthin increased in the WT (Fig. S5*A*), but there was no significant difference in the deepoxidation state (DES) of these xanthophylls (Fig. S5*B*). DES increased within the subsequent 5-min exposure to high light that was used to measure qE. These data indicate that, in parallel to the accumulation of qE-related proteins, acclimation to UV-B induces violaxanthin accumulation, the rapid conversion of which to zeaxanthin upon exposure to high light may enhance qE. A similar accumulation of violaxanthin after exposure to UV-B was also observed in the double mutant *npq4 lhcsr1* (Fig. S5*C*). It is of interest that in the *lhcsr1* and *npq4 lhcsr1* mutants, qE started to develop upon high-light exposure more slowly than in the WT or *npq4* (Fig. S3*A*). One possible interpretation is that a PSBS-dependent component of qE requires the accumulation of zeaxanthin.

We next addressed the regulation of LHCSR1, LHCSR3, and PSBS expression under UV-B. Similar to *Arabidopsis* (16, 19, 21–23, 41), *Chlamydomonas* expresses a homodimeric UVR8 photoreceptor that monomerizes in response to UV-B (Fig. S6) and subsequently

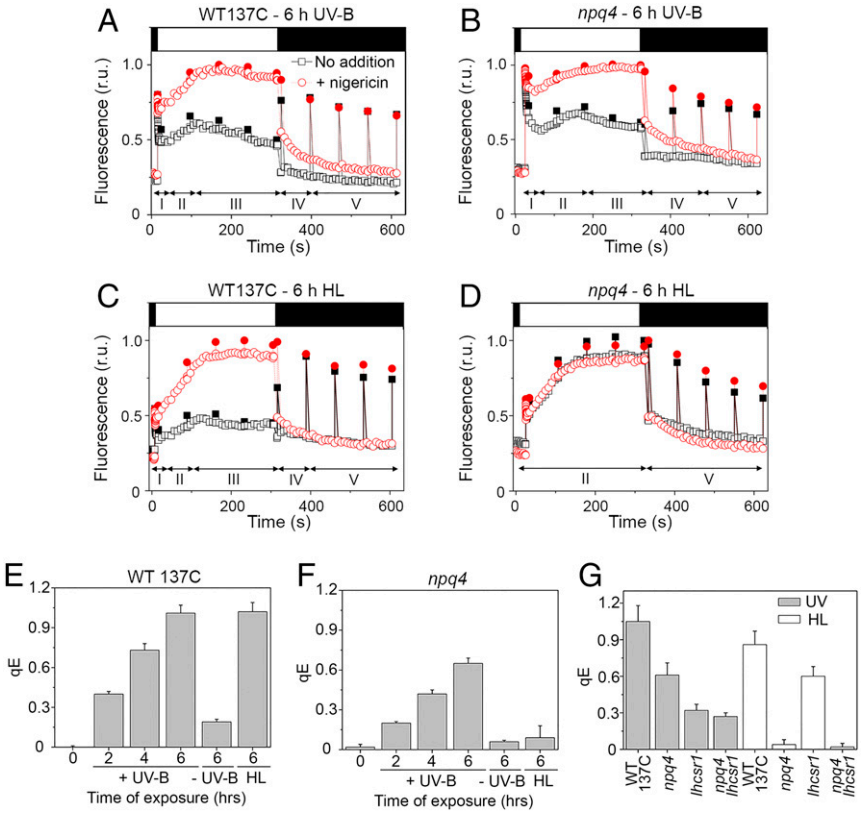

Fig. 2. UV-B induces the capacity for qE. The qE component of NPQ was determined by chlorophyll fluorescence measurements in the presence (red circles) or absence (black squares) of 10 μM nigericin. Dark-adapted cells (black bar at top) were exposed to strong light for 300 s (750 $\mu mol \cdot m^{-2} \cdot s^{-1}$; white bar) and then returned to the dark (dark bar). Fluorescence (relative units; r.u.) was monitored continuously (open symbols) and during saturating flashes (2,500 $\mu mol \cdot m^{-2} \cdot s^{-1}$ at 60-s intervals; filled symbols). (*A* and *B*) WT (WT 137C) (*A*) and *npq4* (*B*) after exposure for 6 h to UV-B. (*C* and *D*) WT (*C*) and *npq4* (*D*) after exposure for 6 h to high light (HL). (*E* and *F*) qE values after 2, 4 or 6 h of exposure to UV-B (+UV-B) or without exposure (−UV-B) and after 6 h of exposure to high light (HL). Means ± SD are shown ($n = 3$) for qE calculated at the end of the actinic light treatment. (*G*) qE values after 6-h exposure of the WT and in mutants *npq4*, *lhcsr1* and *npq4 lhcsr1* to UV-B or to high light (HL). Means ± SD are shown ($n = 4$ for HL; $n = 6$ for UV samples).

interacts with COP1 (32). We obtained a *uvr8* insertional mutant (42) of Chlamydomonas containing no detectable UVR8 protein (Fig. 3*A* and Fig. S6). Expression of UVR8 was partially restored in two independent complementation lines (Fig. 3*A*). The quantum yield of PSII was affected by UV-B in *uvr8* (Fig. 3*C*), indicating a defect in photoprotection. This increased sensitivity was not observed under high light and was rescued in the complemented lines (Fig. 3*C*). Thus, UVR8 regulates an acclimatory response in *Chlamydomonas* specific to UV-B.

uvr8 was defective in the UV-B–induced accumulation of the *PSBS*, *LHCSR1*, and *LHCSR3* transcripts (Fig. 3*D*). Consistently, *uvr8* was also impaired in UV-B–dependent accumulation of the corresponding proteins, but this phenotype was restored in complemented lines (Fig. 3*B*). We further tested whether the induced capacity for qE in response to UV-B depends on UVR8. After UV-B exposure, qE was impaired in *uvr8* and partially restored in the complemented lines (Fig. 3*E* and Fig. S7*A*). This involvement of UVR8 was specific for UV-B responsiveness; in contrast, the *uvr8* mutant still expressed LHCSR3 and a low level of LHCSR1 protein and showed a normal capacity for qE in response to high light (Fig. 3 *E* and *F* and Fig. S7*B*). That the signaling pathways in response to UV-B or high light were different is consistent with our observation that only the latter seems to require photosynthetic electron transport (Fig. 1*C*).

COP1 acts together with UVR8 in UV-B signaling in plants (16, 19, 32, 43). UVR8 monomerization under UV-B was not affected in the *Chlamydomonas* $cop1^{hit1}$ mutant (Fig. S6). However, like *uvr8*, the $cop1^{hit1}$ mutant (44) was also compromised in the UV-B–responsive accumulation of PSBS, LHCSR1, and LHCSR3 proteins (Fig. S8*A*), as well as in the induction of the corresponding transcripts (Fig. S8*B*) (32). Likewise, qE was lower in the $cop1^{hit1}$ mutant than in WT, but was restored in the complemented $cop1^{hit1}$/*COP1* strains (Fig. S8*C*). The data clearly show that qE capacity under UV-B requires the UVR8 photoreceptor and its downstream signaling partner COP1.

We next addressed the physiological relevance of UV-B–enhanced qE capacity for photoprotection against high-light stress. We first compared the extent of photoinhibition under high light of cells that had been acclimated to a low dose of UV-B for 16 h compared with untreated controls. After 60 min of high-light stress treatment, the quantum yield of PSII was 1.13-fold higher in UV-B–acclimated WT cells (F_v/F_m +UV) than in the non-acclimated controls (F_v/F_m –UV) (Fig. 4*A* and Tables S1 and S2). Upon prolonged exposure to high light, the UV-B–acclimated WT culture remained green, whereas the nonacclimated control culture bleached (Fig. 4*B*). In contrast to the WT, the *uvr8* mutant pretreated with UV-B did not show reduced photoinhibition or protection from high-light-induced bleaching (Fig. 4*A, B*). We further tested whether this UVR8-mediated photoprotection from high-light stress can be directly linked to the enhanced qE capacity. Indeed, *npq4* and *lhcsr1* showed less UV-B–induced photoprotection than WT (Fig. 4*C*), and the mutant cultures showed less UV-B acclimation than the WT culture (Fig. 4*D*). Furthermore, the double mutant *npq4 lhcsr1* was even more strongly affected in these acclimation responses (Fig. 4 *C* and *D*). To investigate whether PSBS may also play a role in photoprotection,

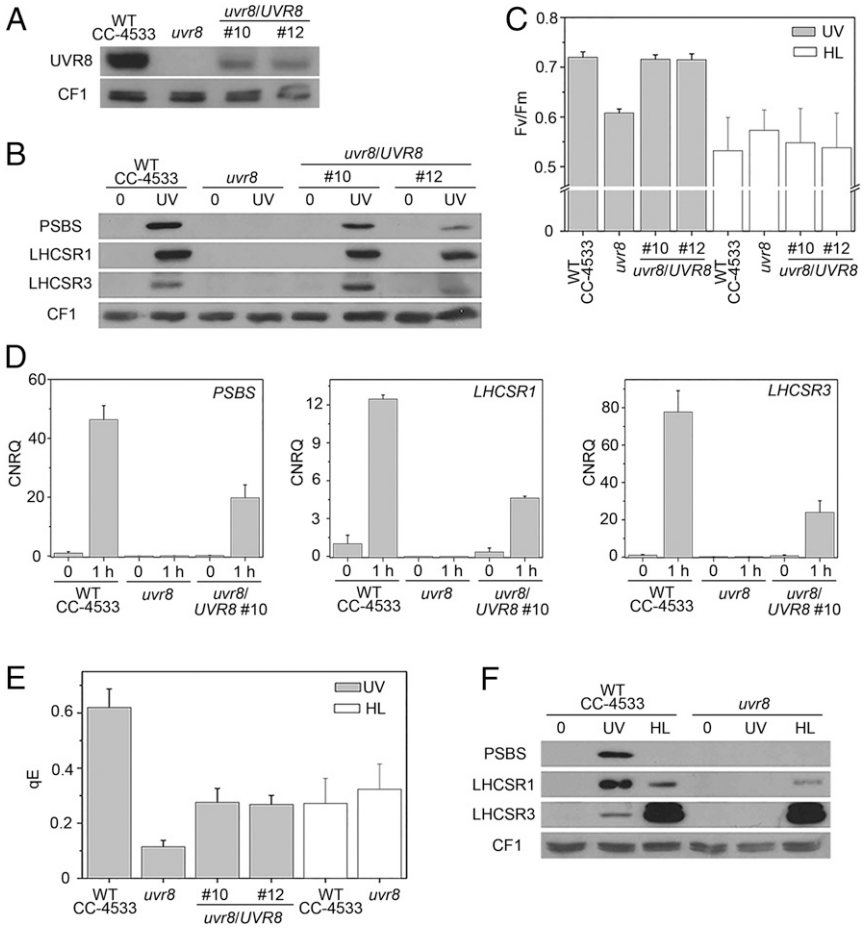

Fig. 3. UVR8 is required for the UV-B response leading to enhanced qE. (*A*) Immunoblot analysis of UVR8 in the WT (WT CC-4533), *uvr8*, and two independent *uvr8*/*UVR8* complemented lines (nos. 10 and 12). (*B*) Immunoblot analysis of PSBS, LHCSR1, and LHCSR3 protein levels in the WT, *uvr8*, and complemented lines in normal growth conditions (0) or after 6-h exposure to UV-B (UV). The ATPase (CF1) levels are shown as loading control. (*C*) The quantum yield of PSII (F_v/F_m) was monitored in the WT, *uvr8*, and complemented strains exposed for 6 h to UV-B or to high light (HL). Note that F_v/F_m of untreated *uvr8* was comparable to WT: *uvr8* = 0.760 ± 0.022; WT = 0.745 ± 0.017; $n = 4$. (*D*) Quantitative RT-PCR analysis of *PSBS*, *LHCSR1*, and *LHCSR3* RNA expression after 1-h UV-B exposure of the WT, *uvr8*, and *uvr8*/*UVR8* complemented line (no. 10). (*E*) qE values in the WT, *uvr8*, and complemented lines (nos. 10 and 12) exposed for 6 h to UV-B or to high light (HL). Note that CC-4533 has a lower qE after HL than the other WT strains used in this work. (*F*) Immunoblot analysis of PSBS, LHCSR1, and LHCSR3 in WT (CC-4533) and *uvr8* in normal growth conditions (0) or after exposure to UV-B (UV) or for 4 h to high light (HL). The ATPase (CF1) levels are shown as loading control.

we compared the *npq4* mutant overexpressing PSBS in the chloroplast with the parental *npq4* strain. Because expression of PSBS in the transformants is constitutive, these experiments were performed without prior exposure to UV-B. Overexpression of PSBS led to a delay in bleaching of the culture under high light and thus contributed to photoprotection (Fig. S4*J*). We conclude that the UVR8-mediated UV-B induction of LHCSR1, LHCSR3, and possibly PSBS markedly contributes to photoprotection under high light.

Conclusion

In *Chlamydomonas*, perception of UV-B photons induces an acclimation response that reduces photodamage to the photosynthesis machinery. This response involves increased accumulation of violaxanthin and also expression of qE-related proteins, mainly LHCSR1 and PSBS, in contrast to LHCSR3, which is induced most in high light (Fig. 4*E*). The UV-B signal appears to act as a proxy for high light, priming the cells for photoprotection. Exposure to high light then rapidly triggers the development of qE and the conversion of violaxanthin to zeaxanthin. The action spectrum of photodamage to the photosynthetic electron transfer chain peaks in UV-B, at wavelengths that are most detrimental to PSII and the manganese cluster involved in water oxidation (33, 34). Thus, predominant expression of LHCSR1 and PSBS under UV-B vs. LHCSR3 under high light may indicate an evolutionary divergence of the signaling pathways, potentially coupled to differences in the activities of these proteins.

Regulatory loops are known to operate in the chloroplast that adjust photosynthetic activity. The status of the photosynthetic chain, sensed for example through the redox poise of key electron carriers or the pH of the thylakoid lumen, influences target photosynthetic proteins by phosphorylation, the reduction of disulfide bridges, or the protonation of regulatory residues (3, 45). We now demonstrate that the photoreceptor UVR8 and its partner COP1 initiate a signaling pathway under UV-B that induces nuclear gene expression of proteins that are then targeted to the chloroplast, where they are involved in the regulation of photosynthesis. Our findings, together with the recent description of a complementary role for PHOT in high-light activation of LHCSR3 expression (14), add a tier of regulation through anterograde signaling to the better-known feedback mechanisms operating within the chloroplast. In *Arabidopsis*, photoperception of UV-B by UVR8 is also important for the maintenance of photosynthetic competence, but the underlying mechanism in higher plants is not clear (35). It will be crucial for agricultural productivity and the biotechnological exploitation of photosynthetic processes to better understand the

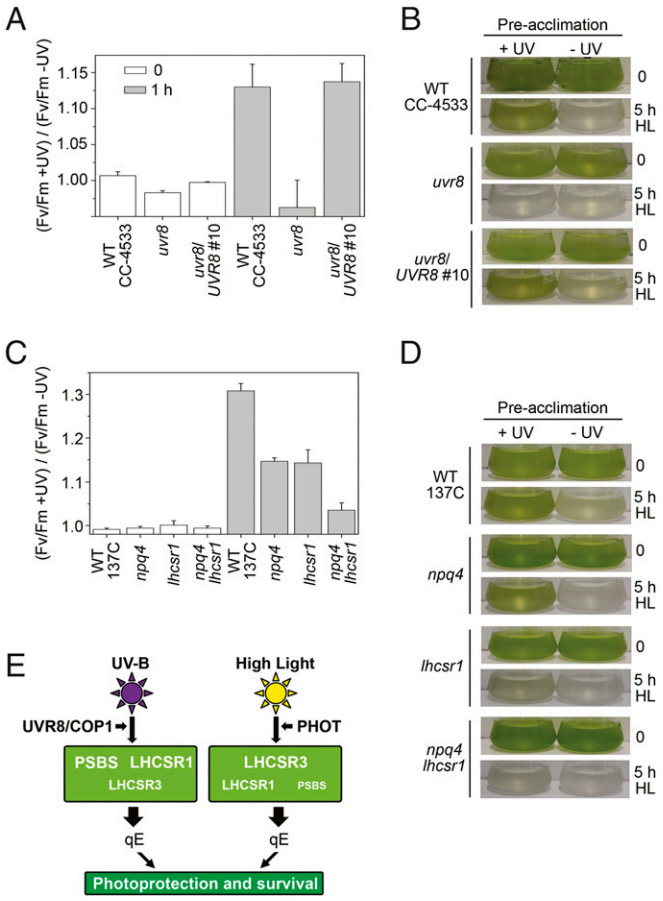

Fig. 4. UV-B acclimation promotes photoprotection. (*A*) The maximum quantum yield of PSII was monitored in cell cultures of WT (WT CC-4533), *uvr8*, and *uvr8*/UVR8 complemented line 10 that had been previously exposed for 16 h to UV-B (F_v/F_m +UV) or were left untreated (F_v/F_m –UV). The effect of acclimation is expressed as the ratio (F_v/F_m +UV)/(F_v/F_m –UV) (error bars represent the SEM; $n = 5$) measured at the end of acclimation (0) and after a subsequent high-light treatment (1 h, 700 μmol·m^{-2}·s^{-1}). (*B*) Cell cultures that had been exposed for 16 h to UV-B (+UV) or untreated controls (–UV) were photographed ($t = 0$) and then exposed to high light (1,000 μmol·m^{-2}·s^{-1}) for 5 h and photographed again ($t = 5$ h). Data shown are representative of three independent biological repetitions. (*C* and *D*) As *A* and *B*, but for the WT (WT 137C) and mutants *npq4*, *lhcsr1*, and *npq4 lhcsr1*. (*C*) Error bars represent the SEM; $n = 3$. (*D*) Data shown are representative of three independent biological repetitions. (*E*) Scheme of photoreceptor-mediated photoprotection of the photosynthetic machinery after UV-B exposure compared with high light.

molecular mechanisms leading to photoprotection and reduced photoinhibition under sunlight and its intrinsic UV-B fraction.

Materials and Methods

Algal Material. The *C. reinhardtii* mutant strains *cop1*^{hit1} (44), *uvr8* (LMJ.RY0402.156289) (42), *npq4* (11), *lhcsr1*, and *npq4 lhcsr1* (7) were used in this work, together with their respective WT background strains, namely, WT137C (mt+) for *npq4*, *lhcsr1*, and *npq4 lhcsr1*; CC-124 (137c mt–) for *cop1*^{hit1}; and CC-4533 (cw15 mt–) for *uvr8*. The *cop1*^{hit1}/*COP1* complementation strains have been described (32).

The UVR8 coding sequence was cloned between the *psaD* promoter and terminator in a Gateway-compatible derivative of pSL18 (46). The *uvr8* mutant was transformed as described (32).

Growth Conditions, UV-B, and High-Light Treatment. Cells were cultivated in Tris acetate phosphate medium under dim light (5–10 μmol·m^{-2}·s^{-1} from fluorescent tubes) at 25 °C. In all experiments, cells were harvested during the exponential phase (1.5–2.5 × 10^6 cells per mL), washed, and resuspended at 2 × 10^7 cells per mL in minimum medium [high-salt medium (HSM)] to favor induction of the capacity for qE (11, 13, 39). They were then acclimated to the new conditions under dim light for 1 h before starting the UV-B or high-light treatments. UV-B treatment (0.2 mW·cm^{-2}) was provided by Philips TL20W/01RS narrowband UV-B tubes under a filter of the WG series (Schott Glaswerke) with half-maximal transmission at 311 nm (21, 32). For the control samples without UV-B treatment (–UV-B), a 360-nm filter was used to block UV-B (<0.001 mW·cm^{-2}). In both cases (+ or – UV-B), cells were concomitantly exposed to dim white light (5 μmol·m^{-2}·s^{-1}; Osram L18W/30 tubes). It should be noted that the low-level UV-B treatment used here causes only minor damage to PSII, as indicated by the maximal quantum yield of PSII in WT 137C, which was 0.76 ± 0.01 ($n = 5$) after 6-h treatment compared with 0.80 ± 0.01 ($n = 5$) in the untreated control. For high-light treatment, cells were exposed under 350 μmol·m^{-2}·s^{-1} white light (fluorescent tubes Osram Dulux L) for 6 h, but only 4 h for WT CC-4533, *uvr8*, and its complemented lines, which are more sensitive.

To determine the effect of UV-B acclimation on subsequent photoprotection, cells (1.5 × 10^6 mL^{-1}) were treated for 16 h under UV-B (0.07 mW·cm^{-2}) as described above. They were then exposed to high light (1,000 μmol·m^{-2}·s^{-1}) with agitation in glass flasks immersed in a water bath at 25 °C.

Protein Extraction and Immunoblot Analysis. Protein extraction and immunoblot analysis were performed as described (32). Anti-CrUVR8 (32), anti-LHCSR3 (47), anti-LHCSR1 (AS14 2819;Agrisera), anti-tubulin (gift from Donald Weeks, University of Nebraska, Lincoln, NE), and anti-CF1 (48) were used. Rabbit polyclonal anti-PSBS antibodies were raised and affinity-purified against the peptide C+AINEGSGKFVDEESA (CrPSBS$^{231–245}$) (Eurogentec), and their specificity was validated by peptide competition assays (Fig. S9); moreover, PSBS was specifically detected in the constitutive PSBS expression lines, but not in the nontransformed control (Fig. S4*E*).

All bands migrate at the position expected for their size: PSBS, 22 kDa; UVR8, 48 kDa (monomer); LHCSR3, 28 kDa (phosphorylated LHCSR3, ∼30 kDa); and LHCSR1, 27 kDa.

Quantitative Real-Time PCR. *Chlamydomonas* RNA was extracted, reverse-transcribed, and analyzed in a 7900HT Real-Time PCR System (Applied Biosystems) as described (32). Expression was normalized to the Cre06.g6364 reference gene (32) and measured in triplicate. The following primers were used: *PSBS* (5′-CCG CCA TCA ACG GCA AGC AG-3′ and 5′-CCA CCA TGG CCA GGC GAC C-3′), *LHCSR1* (5′-AAG ACC CTG CCC GGT GTT AC-3′ and 5′-TGG GTG ATC TCA GAC TCG CGC-3′), *LHCSR3* (5′-GGC CGT CAA GTC CGT GTC T-3′ and 5′-GGG AAG GTT CTT CGT GTA TGC G-3′), and Cre06.g6364 (5′-CTT CTC GCC CAT GAC CAC-3′ and 5′-CCC ACC AGG TTG TTC TTC AG-3′).

qE and Photoinhibition Measurements. NPQ was measured with a video-imaging system (Fluorcam; Photon Systems Instruments). After UV-B or high-light treatment, cells were first briefly adapted to the dark (5 min) and then exposed for 5 min to strong actinic light (750 μmol·m^{-2}·s^{-1}) to monitor the induction of NPQ, and finally returned to the dark to follow its relaxation (Fig. 2 and Fig. S2). Saturating flashes (2,500 μmol·m^{-2}·s^{-1}) at regular intervals allowed a first measurement of maximal chlorophyll fluorescence (F_m) in the initial dark-adapted state and then measurements of maximum fluorescence (F_m') during the exposure to strong light, and subsequent relaxation in the dark (Fig. 2 *A–D*, black peaks; and Fig. S2). The fluorescence in the intervals between the peaks (F_t) was also measured continuously, although this value was not used for the quantitative evaluation of qE.

In *Chlamydomonas*, the qT component (state transition) of NPQ is induced more slowly than the faster qE component. This process results in a complex time course for the maximum fluorescence F_m' peaks (Fig. 2 *A–D* and Fig. S2) (39). The qE component of NPQ, but not the qT component, is entirely dependent on the light-induced acidification of the thylakoid lumen driven by photosynthetic electron flow (12). Therefore, treatment immediately before the fluorescence measurement with the ionophore nigericin (10 μM), which collapses the proton gradient across the thylakoid membrane, inhibits qE (phase I and III) without significantly affecting qT (phase II). Hence, the F_m' time course in the presence of nigericin shows only the qT component: a fluorescence increase toward state 1 in the strong-light phase and a fluorescence decrease toward state 2 in the dark (Fig. S2 and Fig. 2*A*, red curve). The nigericin-sensitive qE component of NPQ can be evaluated at the end of the exposure to strong light by first normalizing the curves to the value of F_m in the absence of nigericin and then subtracting the F_m' peak obtained in the untreated control from that obtained in the presence of nigericin, and normalizing to F_m' [$(F_{m'nig} - F_m')/F_m'$] (39).

To measure the effect of UV-B acclimation on subsequent photoinhibition, cells (1.5 × 10^6 mL^{-1}) were treated for 16 h under UV-B (0.02 mW·cm^{-2}) as above and then exposed to high light for 1 h (700 μmol·m^{-2}·s^{-1}). To monitor

the maximum quantum yield of PSII (using a Plant Efficiency Analyzer from Hansatech), cells were incubated in the dark for 5 min, the fluorescence was measured before (F_o) and during (F_m) a saturating light pulse, and F_v was calculated as $F_m - F_o$.

Transgenic Expression of PSBS from the Chloroplast Genome. The *PSBS1* gene was synthesized by Genscript after chloroplast codon use optimization (Fig. S4 *A* and *B*). The synthetic *PSBS1* gene was cloned into the IR-int vector (49) under the control of the *psaA* promotor (Fig. S4*C*), and the construct was integrated into the *npq4* strain by helium gun bombardment. Transformants were selected for their spectinomycin resistance, and homoplasmicity of the insertions was screened by PCR (Fig. S4*D*).

Pigment Analysis. Carotenoids were analyzed and quantified as described (39, 50).

ACKNOWLEDGMENTS. We thank Martin Jonikas and the *Chlamydomonas* stock center for providing the *uvr8* mutant; Michael Hippler and Dimitris Petroutsos for the anti-LHCSR3 antibody; Donald Weeks for the anti-tubulin antibody; Sabeeha Merchant for the anti-CF1 antibody; Sylvain Loubéry for help with statistical analyses; and Giovanni Finazzi, Michael Hothorn, Dimitris Petroutsos, and Jean-David Rochaix for helpful comments on the manuscript. This work was supported by Swiss National Science Foundation Grants 31003A_153475 (to R.U.) and 31003A_146300 (to M.G.-C.); the European Research Council under the European Union's Seventh Framework Programme (Grant 310539 to R.U.); and the University of Geneva. Construction of the *npq4 lhcsr1* mutant was supported by the U.S. Department of Energy, Office of Science, Basic Energy Sciences, Chemical Sciences, Geosciences, and Biosciences Division under Field Work Proposal 449B. K.K.N. is an investigator for the Howard Hughes Medical Institute and the Gordon and Betty Moore Foundation (through Grant GBMF3070).

1. Li Z, Wakao S, Fischer BB, Niyogi KK (2009) Sensing and responding to excess light. *Annu Rev Plant Biol* 60:239–260.
2. Erickson E, Wakao S, Niyogi KK (2015) Light stress and photoprotection in *Chlamydomonas reinhardtii*. *Plant J* 82(3):449–465.
3. Minagawa J, Tokutsu R (2015) Dynamic regulation of photosynthesis in *Chlamydomonas reinhardtii*. *Plant J* 82(3):413–428.
4. Niyogi KK, Truong TB (2013) Evolution of flexible non-photochemical quenching mechanisms that regulate light harvesting in oxygenic photosynthesis. *Curr Opin Plant Biol* 16(3):307–314.
5. Wobbe L, Bassi R, Kruse O (2016) Multi-level light capture control in plants and green algae. *Trends Plant Sci* 21(1):55–68.
6. Ruban AV (2016) Nonphotochemical chlorophyll fluorescence quenching: Mechanism and effectiveness in protecting plants from photodamage. *Plant Physiol* 170(4): 1903–1916.
7. Ballottari M, et al. (2016) Identification of pH-sensing sites in the Light Harvesting Complex Stress-Related 3 protein essential for triggering non-photochemical quenching in *Chlamydomonas reinhardtii*. *J Biol Chem* 291(14):7334–7346.
8. Bonente G, et al. (2011) Analysis of LhcSR3, a protein essential for feedback de-excitation in the green alga *Chlamydomonas reinhardtii*. *PLoS Biol* 9(1):e1000577.
9. Liguori N, Roy LM, Opacic M, Durand G, Croce R (2013) Regulation of light harvesting in the green alga *Chlamydomonas reinhardtii*: The C-terminus of LHCSR is the knob of a dimmer switch. *J Am Chem Soc* 135(49):18339–18342.
10. Li XP, et al. (2000) A pigment-binding protein essential for regulation of photosynthetic light harvesting. *Nature* 403(6768):391–395.
11. Peers G, et al. (2009) An ancient light-harvesting protein is critical for the regulation of algal photosynthesis. *Nature* 462(7272):518–521.
12. Niyogi KK, Bjorkman O, Grossman AR (1997) *Chlamydomonas* xanthophyll cycle mutants identified by video imaging of chlorophyll fluorescence quenching. *Plant Cell* 9(8):1369–1380.
13. Petroutsos D, et al. (2011) The chloroplast calcium sensor CAS is required for photoacclimation in *Chlamydomonas reinhardtii*. *Plant Cell* 23(8):2950–2963.
14. Petroutsos D, et al. (2016) A blue-light photoreceptor mediates the feedback regulation of photosynthesis. *Nature* 537(7621):563–566.
15. Jenkins GI (2009) Signal transduction in responses to UV-B radiation. *Annu Rev Plant Biol* 60:407–431.
16. Heijde M, Ulm R (2012) UV-B photoreceptor-mediated signalling in plants. *Trends Plant Sci* 17(4):230–237.
17. Jansen MAK, Gaba V, Greenberg BM (1998) Higher plants and UV-B radiation: Balancing damage, repair and acclimation. *Trends Plant Sci* 3(4):131–135.
18. Kliebenstein DJ, Lim JE, Landry LG, Last RL (2002) *Arabidopsis* UVR8 regulates ultraviolet-B signal transduction and tolerance and contains sequence similarity to human regulator of chromatin condensation 1. *Plant Physiol* 130(1):234–243.
19. Favory JJ, et al. (2009) Interaction of COP1 and UVR8 regulates UV-B-induced photomorphogenesis and stress acclimation in *Arabidopsis*. *EMBO J* 28(5):591–601.
20. González Besteiro MA, Bartels S, Albert A, Ulm R (2011) *Arabidopsis* MAP kinase phosphatase 1 and its target MAP kinases 3 and 6 antagonistically determine UV-B stress tolerance, independent of the UVR8 photoreceptor pathway. *Plant J* 68(4): 727–737.
21. Rizzini L, et al. (2011) Perception of UV-B by the *Arabidopsis* UVR8 protein. *Science* 332(6025):103–106.
22. Christie JM, et al. (2012) Plant UVR8 photoreceptor senses UV-B by tryptophan-mediated disruption of cross-dimer salt bridges. *Science* 335(6075):1492–1496.
23. Wu D, et al. (2012) Structural basis of ultraviolet-B perception by UVR8. *Nature* 484(7393):214–219.
24. Kaiserli E, Jenkins GI (2007) UV-B promotes rapid nuclear translocation of the *Arabidopsis* UV-B specific signaling component UVR8 and activates its function in the nucleus. *Plant Cell* 19(8):2662–2673.
25. Yin R, Arongaus AB, Binkert M, Ulm R (2015) Two distinct domains of the UVR8 photoreceptor interact with COP1 to initiate UV-B signaling in *Arabidopsis*. *Plant Cell* 27(1):202–213.
26. Brown BA, et al. (2005) A UV-B-specific signaling component orchestrates plant UV protection. *Proc Natl Acad Sci USA* 102(50):18225–18230.
27. Binkert M, et al. (2014) UV-B-responsive association of the *Arabidopsis* bZIP transcription factor ELONGATED HYPOCOTYL5 with target genes, including its own promoter. *Plant Cell* 26(10):4200–4213.
28. Yin R, Skvortsova MY, Loubéry S, Ulm R (2016) COP1 is required for UV-B-induced nuclear accumulation of the UVR8 photoreceptor. *Proc Natl Acad Sci USA* 113(30): E4415–E4422.
29. Huang X, et al. (2013) Conversion from CUL4-based COP1-SPA E3 apparatus to UVR8-COP1-SPA complexes underlies a distinct biochemical function of COP1 under UV-B. *Proc Natl Acad Sci USA* 110(41):16669–16674.
30. Heijde M, Ulm R (2013) Reversion of the *Arabidopsis* UV-B photoreceptor UVR8 to the homodimeric ground state. *Proc Natl Acad Sci USA* 110(3):1113–1118.
31. Heilmann M, Jenkins GI (2013) Rapid reversion from monomer to dimer regenerates the ultraviolet-B photoreceptor UV RESISTANCE LOCUS8 in intact *Arabidopsis* plants. *Plant Physiol* 161(1):547–555.
32. Tilbrook K, et al. (2016) UV-B perception and acclimation in *Chlamydomonas reinhardtii*. *Plant Cell* 28(4):966–983.
33. Takahashi S, et al. (2010) The solar action spectrum of photosystem II damage. *Plant Physiol* 153(3):988–993.
34. Zavafer A, Chow WS, Cheah MH (2015) The action spectrum of photosystem II photoinactivation in visible light. *J Photochem Photobiol B* 152(Pt B):247–260.
35. Davey MP, et al. (2012) The UV-B photoreceptor UVR8 promotes photosynthetic efficiency in *Arabidopsis thaliana* exposed to elevated levels of UV-B. *Photosynth Res* 114(2):121–131.
36. Tibiletti T, Auroy P, Peltier G, Caffarri S (2016) *Chlamydomonas reinhardtii* PsbS protein is functional and accumulates rapidly and transiently under high light. *Plant Physiol* 171(4):2717–2730.
37. Correa-Galvis V, et al. (2016) Photosystem II subunit PsbS is involved in the induction of LHCSR protein-dependent energy dissipation in *Chlamydomonas reinhardtii*. *J Biol Chem* 291(33):17478–17487.
38. Maruyama S, Tokutsu R, Minagawa J (2014) Transcriptional regulation of the stress-responsive light harvesting complex genes in *Chlamydomonas reinhardtii*. *Plant Cell Physiol* 55(7):1304–1310.
39. Allorent G, et al. (2013) A dual strategy to cope with high light in *Chlamydomonas reinhardtii*. *Plant Cell* 25(2):545–557.
40. Dinc E, et al. (2016) LHCSR1 induces a fast and reversible pH-dependent fluorescence quenching in LHCII in *Chlamydomonas reinhardtii* cells. *Proc Natl Acad Sci USA* 113(27):7673–7678.
41. Jenkins GI (2014) Structure and function of the UV-B photoreceptor UVR8. *Curr Opin Struct Biol* 29:52–57.
42. Li X, et al. (2016) An indexed, mapped mutant library enables reverse genetics studies of biological processes in *Chlamydomonas reinhardtii*. *Plant Cell* 28(2):367–387.
43. Oravecz A, et al. (2006) CONSTITUTIVELY PHOTOMORPHOGENIC1 is required for the UV-B response in Arabidopsis. *Plant Cell* 18(8):1975–1990.
44. Schierenbeck L, et al. (2015) Fast forward genetics to identify mutations causing a high light tolerant phenotype in *Chlamydomonas reinhardtii* by whole-genome-sequencing. *BMC Genomics* 16(1):57.
45. Serrato AJ, Fernández-Trijueque J, Barajas-López JD, Chueca A, Sahrawy M (2013) Plastid thioredoxins: A "one-for-all" redox-signaling system in plants. *Front Plant Sci* 4:463.
46. Depège N, Bellafiore S, Rochaix JD (2003) Role of chloroplast protein kinase Stt7 in LHCII phosphorylation and state transition in *Chlamydomonas*. *Science* 299(5612): 1572–1575.
47. Naumann B, et al. (2007) Comparative quantitative proteomics to investigate the remodeling of bioenergetic pathways under iron deficiency in *Chlamydomonas reinhardtii*. *Proteomics* 7(21):3964–3979.
48. Hamel PP, Dreyfuss BW, Xie Z, Gabilly ST, Merchant S (2003) Essential histidine and tryptophan residues in CcsA, a system II polytopic cytochrome c biogenesis protein. *J Biol Chem* 278(4):2593–2603.
49. Michelet L, Lefebvre-Legendre L, Burr SE, Rochaix JD, Goldschmidt-Clermont M (2011) Enhanced chloroplast transgene expression in a nuclear mutant of *Chlamydomonas*. *Plant Biotechnol J* 9(5):565–574.
50. Fraser PD, Pinto ME, Holloway DE, Bramley PM (2000) Technical advance: Application of high-performance liquid chromatography with photodiode array detection to the metabolic profiling of plant isoprenoids. *Plant J* 24(4):551–558.